

NOTES AND CORRESPONDENCE

Rapid Scan Views of Convectively Generated Mesovortices in Sheared Tropical Cyclone Gustav (2002)

ERIC A. HENDRICKS

Department of Atmospheric Science, Colorado State University, Fort Collins, Colorado

MICHAEL T. MONTGOMERY

Department of Meteorology, Naval Postgraduate School, Monterey, California, and NOAA/AOML/Hurricane Research Division, Miami, Florida

(Manuscript received 1 June 2004, in final form 2 March 2006)

ABSTRACT

On 9–10 September 2002, multiple mesovortices were captured in great detail by rapid scan visible satellite imagery in subtropical, then later, Tropical Storm Gustav. These mesovortices were observed as low-level cloud swirls while the low-level structure of the storm was exposed due to vertical shearing. They are shown to form most plausibly via vortex tube stretching associated with deep convection; they become decoupled from the convective towers by vertical shear; they are advected with the low-level circulation; finally they initiate new hot towers on their boundaries. Partial evidence of an axisymmetrizing mesovortex and its hypothesized role in the parent vortex spinup is presented. Observations from the mesoscale and synoptic scale are synthesized to provide a multiscale perspective of the intensification of Gustav that occurred on 10 September. The most important large-scale factors were the concurrent relaxation of the 850–200-hPa-deep layer vertical wind shear from 10–15 to 5–10 m s^{-1} and movement over pockets of very warm sea surface temperatures (approximately 29.5°–30.5°C). The mesoscale observations are not sufficient alone to determine the precise role of the deep convection and mesovortices in the intensification. However, qualitative comparisons are made between the mesoscale processes observed in Gustav and recent full-physics and idealized numerical simulations to obtain additional insight.

1. Introduction

Two major forecasting difficulties with tropical cyclones are genesis and intensification. Forecast skill for these processes has consistently lagged forecast skill for track over the years (e.g., Sheets 1990). While general favorable (sea surface temperatures greater than 26°C, moist midtroposphere, and presence of a preexisting disturbance) and unfavorable (particularly strong vertical wind shear) synoptic-scale conditions affecting these processes have been well known for some time (e.g., Gray 1968), significantly less is known about the

intrinsic storm-scale dynamical and convective processes that affect genesis and intensification.

Recent studies of near-cloud-resolving numerical simulations run at a horizontal grid spacing of 2–3 km have added new clarity to these processes. Montgomery et al. (2006, hereafter MNCS) demonstrated that the incipient surface vortex could be built by small-scale cores of rotating deep convection (so-called vortical hot towers, hereafter VHTs) via the coalescence and system-scale concentration of their convectively generated cyclonic vorticity anomalies in an idealized framework. Hendricks et al. (2004, hereafter HMD) demonstrated a similar genesis pathway in a real storm, Hurricane Diana (in 1984). However, the lack of dense in situ measurements combined with cirrus cloud canopies that tend to obscure the low-level storm structure have limited the ability to assess these and other numerical model simulations.

Corresponding author address: Eric A. Hendricks, Dept. of Atmospheric Science, Colorado State University, Fort Collins, CO 80523.

E-mail: eric.hendricks@gmail.com

| Report Documentation Page | | | | Form Approved OMB No. 0704-0188 | |
|--|------------------------------------|-------------------------------------|---|---|---------------------------------|
| Public reporting burden for the collection of information is estimated to average 1 hour per response, including the time for reviewing instructions, searching existing data sources, gathering and maintaining the data needed, and completing and reviewing the collection of information. Send comments regarding this burden estimate or any other aspect of this collection of information, including suggestions for reducing this burden, to Washington Headquarters Services, Directorate for Information Operations and Reports, 1215 Jefferson Davis Highway, Suite 1204, Arlington VA 22202-4302. Respondents should be aware that notwithstanding any other provision of law, no person shall be subject to a penalty for failing to comply with a collection of information if it does not display a currently valid OMB control number. | | | | | |
| 1. REPORT DATE MAR 2006 | | 2. REPORT TYPE | | 3. DATES COVERED 00-00-2006 to 00-00-2006 | |
| 4. TITLE AND SUBTITLE Rapid Scan Views of Convectively Generated Mesovortices in Sheared Tropical Cyclone Gustav (2002) | | | | 5a. CONTRACT NUMBER | |
| | | | | 5b. GRANT NUMBER | |
| | | | | 5c. PROGRAM ELEMENT NUMBER | |
| 6. AUTHOR(S) | | | | 5d. PROJECT NUMBER | |
| | | | | 5e. TASK NUMBER | |
| | | | | 5f. WORK UNIT NUMBER | |
| 7. PERFORMING ORGANIZATION NAME(S) AND ADDRESS(ES) Naval Postgraduate School, Department of Meteorology, Monterey, CA, 93943 | | | | 8. PERFORMING ORGANIZATION REPORT NUMBER | |
| 9. SPONSORING/MONITORING AGENCY NAME(S) AND ADDRESS(ES) | | | | 10. SPONSOR/MONITOR'S ACRONYM(S) | |
| | | | | 11. SPONSOR/MONITOR'S REPORT NUMBER(S) | |
| 12. DISTRIBUTION/AVAILABILITY STATEMENT Approved for public release; distribution unlimited | | | | | |
| 13. SUPPLEMENTARY NOTES | | | | | |
| 14. ABSTRACT On 9?10 September 2002, multiple mesovortices were captured in great detail by rapid scan visible satellite imagery in subtropical, then later, Tropical Storm Gustav. These mesovortices were observed as low-level cloud swirls while the low-level structure of the storm was exposed due to vertical shearing. They are shown to form most plausibly via vortex tube stretching associated with deep convection; they become decoupled from the convective towers by vertical shear; they are advected with the low-level circulation finally they initiate new hot towers on their boundaries. Partial evidence of an axisymmetrizing mesovortex and its hypothesized role in the parent vortex spinup is presented. Observations from the mesoscale and synoptic scale are synthesized to provide a multiscale perspective of the intensification of Gustav that occurred on 10 September. The most important large-scale factors were the concurrent relaxation of the 850?200-hPa-deep layer vertical wind shear from 10?15 to 5?10 m s⁻¹ and movement over pockets of very warm sea surface temperatures (approximately 29.5??30.5°C). The mesoscale observations are not sufficient alone to determine the precise role of the deep convection and mesovortices in the intensification. However qualitative comparisons are made between the mesoscale processes observed in Gustav and recent fullphysics and idealized numerical simulations to obtain additional insight. | | | | | |
| 15. SUBJECT TERMS | | | | | |
| 16. SECURITY CLASSIFICATION OF: | | | 17. LIMITATION OF ABSTRACT Same as Report (SAR) | 18. NUMBER OF PAGES 10 | 19a. NAME OF RESPONSIBLE PERSON |
| a. REPORT unclassified | b. ABSTRACT unclassified | c. THIS PAGE unclassified | | | |

Tropical Cyclone Gustav presented a unique opportunity to “look into” a developing tropical system and observe the low-level structure. The eastern portion of the storm was exposed on 9 September due to moderate easterly vertical shear, uncovering multiple mesovortices that were present. Areas of the storm were also exposed on 10 September, and more of these mesovortices were visible. The evolution of these mesovortices was captured with the rapid scan visible satellite imagery.

Gustav was of the class of storms that made a transition from an ordinary baroclinic cyclone to a warm-core tropical storm (tropical transition, TT; Davis and Bosart 2003, 2004, hereafter DB03, DB04, respectively). This is in contrast to the well-known extratropical transition that occurs when tropical cyclones move into the higher latitudes (typically greater than 30°N). Tropical transition is physically defined as the morphing of a cold-core cyclone with baroclinic origins into a warm-core surface-based tropical cyclone (DB04). In the TT classification system of DB04, Gustav was considered initially to be a strong extratropical cyclone. In such cases, the frontal cyclone may gain sufficient strength to trigger a wind-induced surface heat exchange amplification process (WISHE; Emanuel et al. 1994). According to DB04, the TT happens via diabatic convective processes that tend to erode the preexisting vertical wind shear and produce a warm core (cf. Montgomery and Farrell, 1993).

While the main focus of this note will be a detailed illustration of the structure and evolution of the mesovortices, the observational data and Quick Scatterometer (QuikSCAT) near-surface winds will be used to provide a multiscale perspective of the tropical transition that occurred. Insights into potential mechanisms of the tropical transition (DB03) will be discussed in light of this observational study.

2. Synoptic history: 8–12 September 2002

A detailed synoptic history of Tropical Storm Gustav was provided by the National Hurricane Center (NHC) in Miami, Florida (Beven 2005). A brief summary of that report is provided here. The incipient storm formed from an area of disturbed weather between the Bahamas and Bermuda on 6 September 2002, in association with a trough. Late on 7 September 2002, a broad surface low formed in the area of disturbed weather. By 1200 UTC 8 September, the surface low was classified as a subtropical depression and was located approximately 815 km south-southeast of Cape Hatteras, North Carolina. Later that day, an Air Force Reserve Hurricane Hunter aircraft investigated the cy-

clone and found it had become subtropical storm Gustav.

On 9 September, Gustav moved erratically west-northwestward and slowly intensified. Gustav turned north early on 10 September and the convection became better organized near the center. The system was classified as a tropical storm (TS) by the NHC at 1200 UTC 10 September based on the development of strong winds close to its center. As the center of Gustav reached Cape Hatteras, the maximum sustained winds increased to 28 m s^{-1} . The storm continued to intensify after interacting with an upper-level low pressure system and became the first hurricane of the 2002 Atlantic hurricane season at 1200 UTC 11 September. Gustav made landfall as a hurricane in Nova Scotia at 0430 UTC 12 September. After this, observations indicated that the storm was beginning to lose its tropical characteristics. Gustav lost all tropical characteristics by approximately 1200 UTC 12 September near Newfoundland.

3. Data and analysis procedures

The observational products used are rapid scan visible satellite imagery, National Centers for Environmental Prediction–National Center for Atmospheric Research (NCEP–NCAR) reanalysis data (Kalnay et al. 1996; Kistler et al. 2001), and microwave scatterometer data.

The visible imagery (channel 1; $\lambda = 0.65 \mu\text{m}$) is obtained from the *Geostationary Operational Environmental Satellite-8 (GOES-8)* storm floater on 9–10 September 2002. The approximate horizontal resolution is 1 km. The satellite was scanning in the Rapid Scan Operating (RSO) mode, with satellite images produced in 7.5-min intervals. Gridded data are obtained from the National Aeronautics and Space Administration (NASA) SeaWinds scatterometer on board the QuikSCAT satellite during 9–10 September 2002. (More detail on the scatterometer can be found in the appendix.) The dataset contains scatterometer-derived zonal and meridional vector components of the near-surface winds for a morning ascending pass and evening descending pass of the satellite over the region where Gustav developed. The NCEP–NCAR reanalysis 6-hourly composite data are used for analysis of the larger-scale environment, namely, vertical wind shear, thermodynamic profiles, and atmospheric moisture. The reanalysis data resolution is 2.5° by 2.5° (latitude by longitude). While this resolution is somewhat coarse, it is sufficient to broadly capture the evolution of the large-scale fields in the vicinity of Gustav.

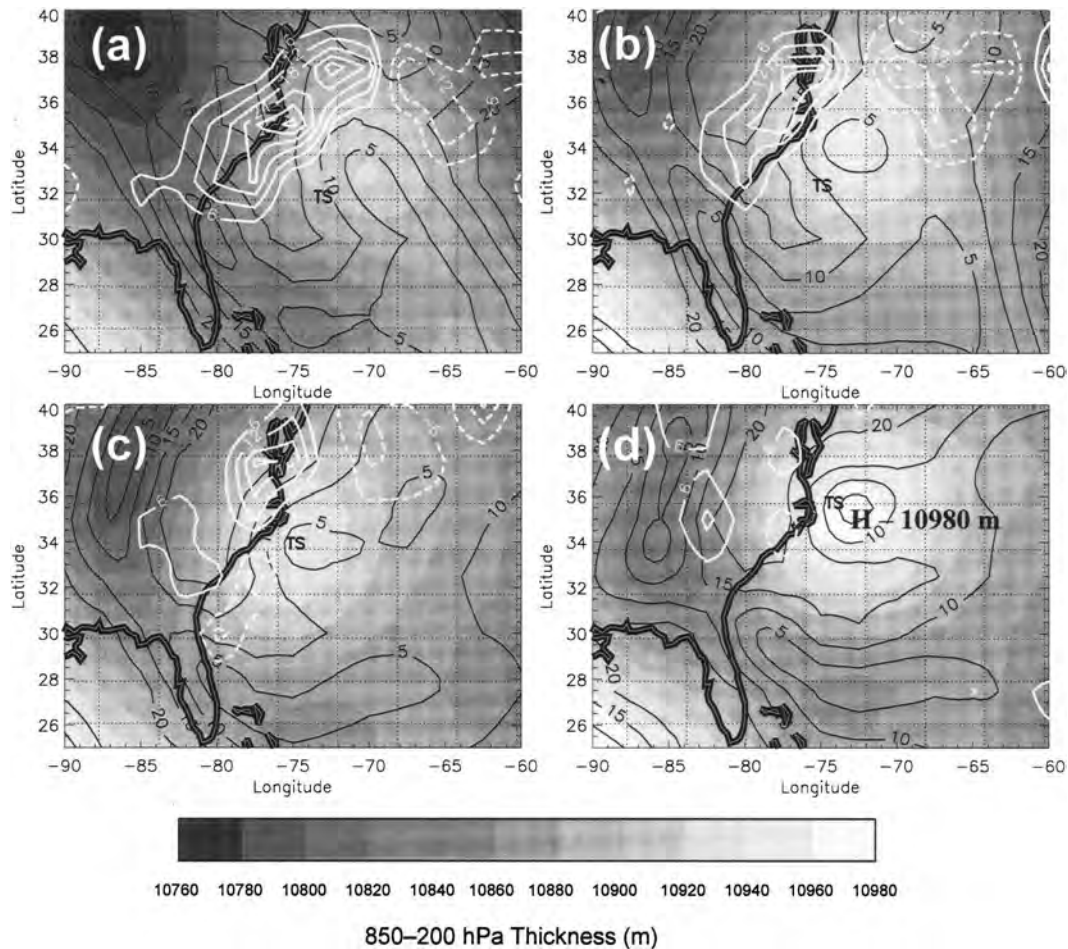


FIG. 1. Evolution of low-level moisture advection, deep-layer vertical wind shear, and thickness. Moisture advection is calculated at 1000 hPa and displayed with white contours [$\text{g kg}^{-1} (12 \text{ h})^{-1}$], the 850–200-hPa vertical wind shear is plotted in the solid black lines (m s^{-1}), and the 850–200-hPa thickness is shaded, with increasing heights as lighter shades (interval is 20 m): (a) 1200 UTC 9 Sep, (b) 0000 UTC 10 Sep, (c) 1200 UTC 10 Sep, and (d) 0000 UTC 11 Sep 2002. The NHC best-track position of Gustav is marked with a TS symbol.

4. Synoptic-scale analysis

a. Thickness, vertical wind shear, and moisture advection

The evolution of the 850–200-hPa thickness, the 850–200-hPa vertical wind shear, and the 1000-hPa horizontal moisture advection are shown in Fig. 1 at 1200 and 0000 UTC 9–10 September. The fields are calculated from 6-hourly NCEP–NCAR reanalysis data composites. The thickness is calculated by the difference between geopotential heights of the 200- and 850-hPa pressure levels. The vertical wind shear is expressed by the magnitude of the difference between the horizontal velocity vectors at the 200- and 850-hPa levels. The moisture advection is calculated from the specific humidity q and horizontal velocity vector \mathbf{V} from the re-

analysis data, $-\mathbf{V} \cdot \nabla q$, at the surface, and displayed in 12-h tendencies.

At 1200 UTC 9 September (Fig. 1a), the storm was in a region of deep-layer shear between 10 and 15 m s^{-1} . The low-level center (marked by the TS) was southwest of the warm thickness center. The geostrophic vertical wind shear was approximately from the east-southeast (using thermal wind) as shown by the thickness field associated with the warm thickness center north of the storm. The strongest moisture advection was northwest of the storm at this time. Progressing to 0000 UTC 11 September (Fig. 1d), the main changes in the synoptic environment were as follows: 1) the warm thickness ridge became stronger, 2) the shear weakened to less than 10 m s^{-1} , and 3) the low-level center became more aligned with the warm thickness center. At 1200 UTC

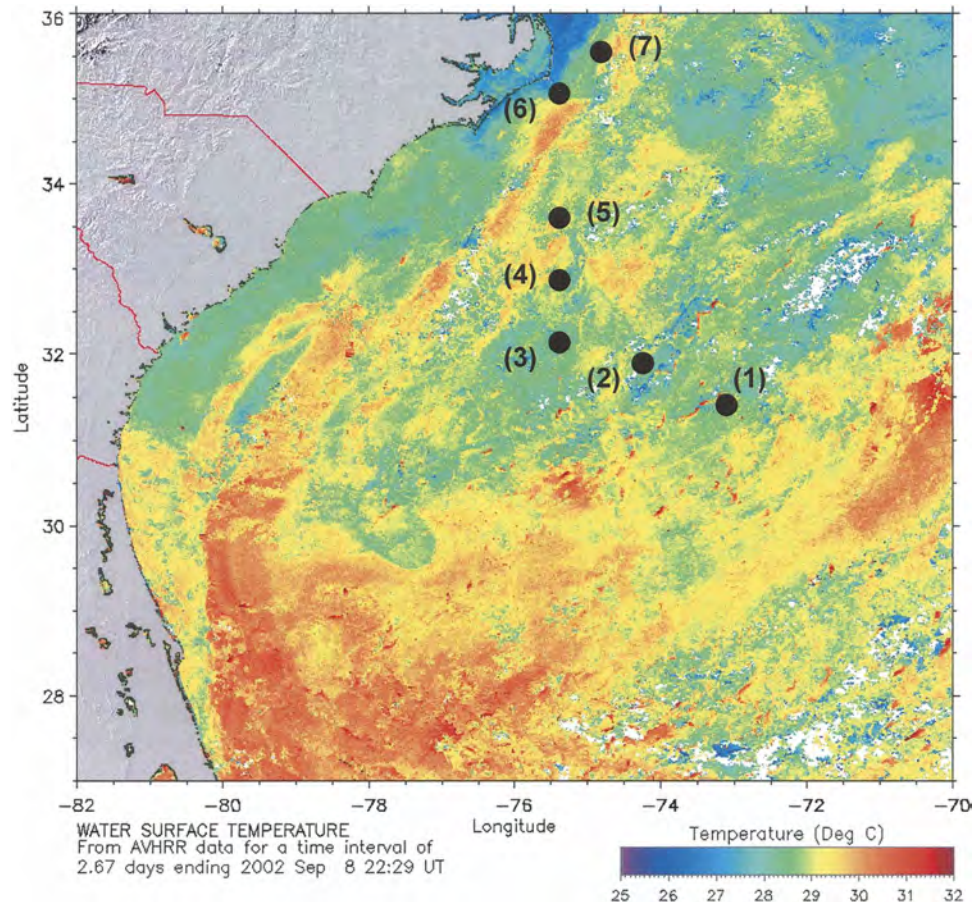


FIG. 2. SSTs ($^{\circ}\text{C}$) in the region where Gustav formed from the AVHRR on board the NOAA polar-orbiting satellites. The NHC best-track position of the storm is marked by black circles: 1) 1200 UTC 9 Sep (31.6°N , 73.6°W), 2) 1800 UTC 9 Sep (31.9°N , 74.5°W), 3) 0000 UTC 10 Sep (32.1°N , 75.5°W), 4) 0600 UTC 10 Sep (33.0°N , 75.5°W), 5) 1200 UTC 10 Sep (33.7°N , 75.4°W), 6) 1800 UTC 10 Sep (35.0°N , 75.4°W), and 7) 0000 UTC 11 Sep 2002 (35.5°N , 74.7°W). (Figure is courtesy of the Johns Hopkins University Applied Physics Laboratory.)

10 September (12 h earlier), the synoptic environment appeared to be even more favorable, with total shear of less than 5 m s^{-1} over the storm.

b. Sea surface temperature

A detailed composite of sea surface temperatures (SSTs) from the Advanced Very High Resolution Radiometer (AVHRR) on the National Oceanic and Atmospheric Administration (NOAA) polar-orbiting satellites in the region of Gustav is shown in Fig. 2 at 2215 UTC 8 September 2002. The SSTs were shown at this time since the storm had not yet moved over the region, and they are therefore indicative of the environment into which the storm was heading (nor were the waters cooled by any previous system before Gustav). SSTs ranged from 28° to 29°C in the storm vicinity, although small areas of higher temperatures (up to approximately 29.5° – 30.5°C) were seen as well.

From 1200 UTC 9 September to 0000 UTC 10 September (positions 1, 2, and 3), the storm was over waters of approximately 28° – 29°C . From 0600 UTC 10 September to 0000 UTC 11 September (positions 4, 5, 6, and 7), the storm moved over the warmer pockets (29.5° – 30.5°C) associated with the Gulf Stream. Excluding other factors, these higher SSTs would have promoted further intensification.

c. Near-surface winds and vorticity derived from QuikSCAT

Four passes of QuikSCAT occurred on 9–10 September. The passes were approximately 12 h apart and include a morning ascending pass and evening descending pass on each day. The scatterometer-derived near-surface wind barbs and absolute vertical vorticity for each pass are shown in Fig. 3. The direction of satellite movement and the time of the pass are also shown in

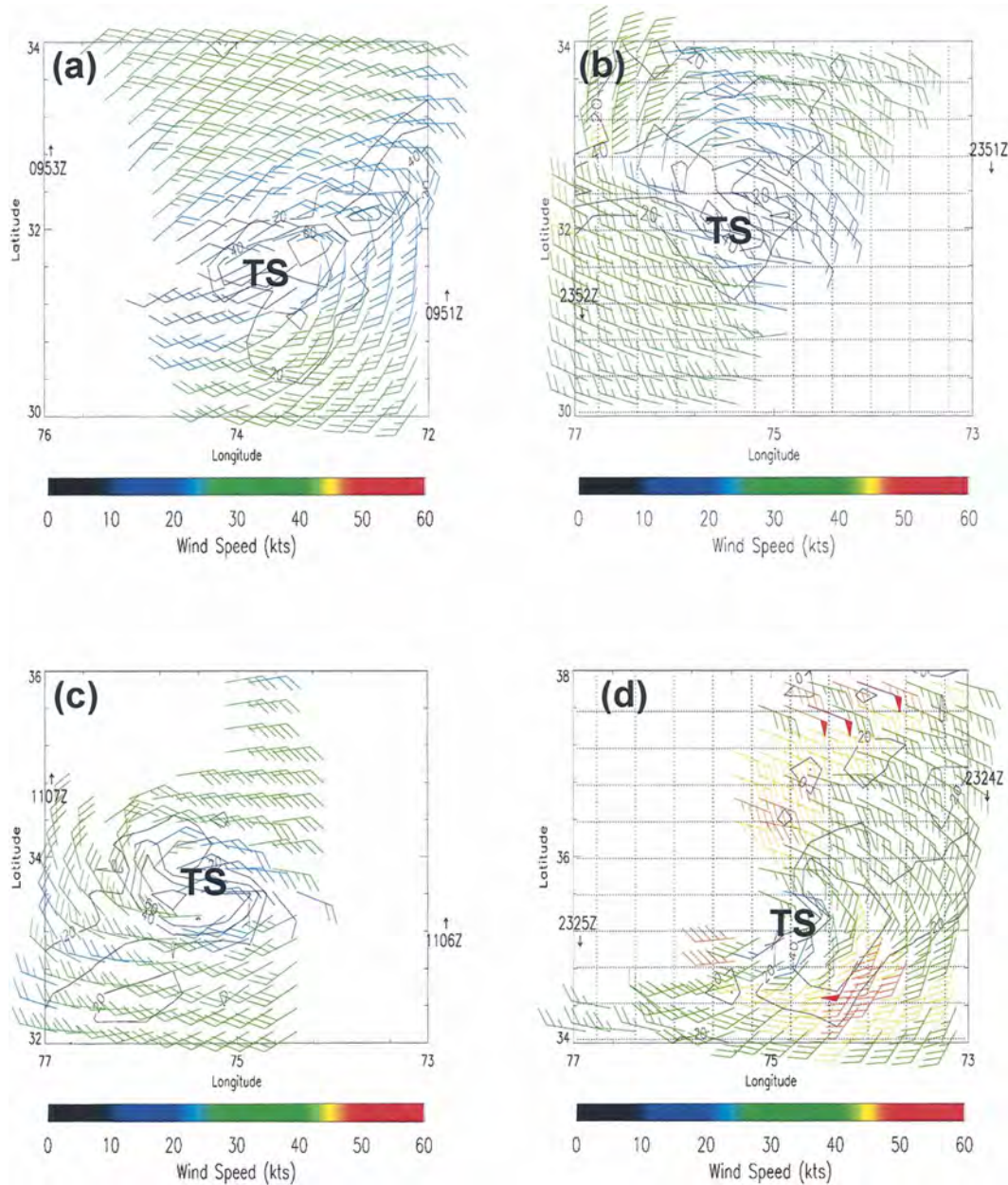


FIG. 3. Near-surface wind barbs and absolute vertical vorticity (10^{-5} s^{-1}) derived from the QuikSCAT scatterometer during 9–10 Sep 2002 (each contour represents an interval of $20 \times 10^{-5} \text{ s}^{-1}$): (a) ascending pass at 0950 UTC 9 Sep, (b) descending pass at 2350 UTC 9 Sep, (c) ascending pass at 1106 UTC 10 Sep, and (d) descending pass at 2325 UTC 10 Sep 2002. The NHC best-track storm center fix is marked by the TS symbol. The direction of satellite movement and the UTC time of the eastern and western edges of the pass are also marked in the plot.

each plot. Absolute vertical vorticity was calculated with the zonal u and meridional v QuikSCAT wind components and the planetary vorticity, that is, $f + dv/dx - du/dy$, with $dx = dy = 25 \text{ km}$. In precipitating regions in tropical cyclone (TC) cores, QuikSCAT is known to be less reliable. At certain times the shape of the TC vortex appears elliptical in Fig. 3. It is not

known whether this shape is real or if it is caused by some erroneous QuikSCAT winds in the precipitating regions of the storm.

At 0950 UTC 9 September, a cyclonic circulation existed with wind speeds generally between 10 and 15 m s^{-1} . By 2351 UTC, some moderate strengthening was seen on the western side of the center (Fig. 3b, marked

by the TS) (winds approximately $15\text{--}20\text{ m s}^{-1}$), while winds were more or less steady elsewhere. At 1106 UTC 10 September, the area of stronger winds was gone, and generally, maximum winds were approximately $10\text{--}15\text{ m s}^{-1}$. In the final pass, significant strengthening of the storm was observed; low-level winds increased to approximately $15\text{--}25\text{ m s}^{-1}$. The QuikSCAT data indicate that Gustav was not changing significantly in intensity on 9 September, and then it began to intensify on 10 September, particularly after 1200 UTC. The peak absolute vertical vorticity was approximately $60 \times 10^{-5}\text{ s}^{-1}$ on 9 September (both passes; Fig. 3a and 3b). The 1107 UTC 10 September pass (Fig. 3c) yielded the largest peak absolute vorticity, $80 \times 10^{-5}\text{ s}^{-1}$. The peak values on the final pass on that day were smaller, $40 \times 10^{-5}\text{ s}^{-1}$. QuikSCAT winds (and vorticity) were not available on the western portion of the storm at this time since this area was over land (North Carolina). The larger values in Fig. 3c may be a signature of one of the mesovortices on 10 September (see section 5c). However, due to the coarse QuikSCAT resolution of 25 km, the mesovortex vorticity is not resolved. In comparison to the NHC best-track intensity estimate, QuikSCAT near-surface winds were slightly lower throughout this period. The NHC best-track intensities were 21 m s^{-1} (1200 UTC 9 September), 23 m s^{-1} (0000 UTC 10 September), 26 m s^{-1} (1200 UTC 10 September), and 28 m s^{-1} (0000 UTC 11 September).

d. Discussion

Based on the analysis above, it is concluded that the synoptic environment became more favorable on 10 September. The main favorable changes were the concurrent relaxing of the 850–200-hPa vertical wind shear from $10\text{--}15$ to $5\text{--}10\text{ m s}^{-1}$ combined with storm movement over very warm waters. The moisture advection was maximized northwest of the storm center, and was likely the primary contributor to the sustained deep convective activity in that area. According to DB04, the environmental vertical wind shear can be reduced in subtropical storms such as Gustav by diabatic processes in sustained deep convection. It is possible that the vertical wind shear reduction that occurred in Gustav may have proceeded via this pathway. However, we also cannot rule out the shear reduction being caused by the evolving large-scale environment.

The relatively high 850–200-hPa thickness values over the storm indicate that the cold-core system had already eroded substantially by 9 September. However, the movement of the surface low beneath the warm thickness center did not occur until approximately 1200

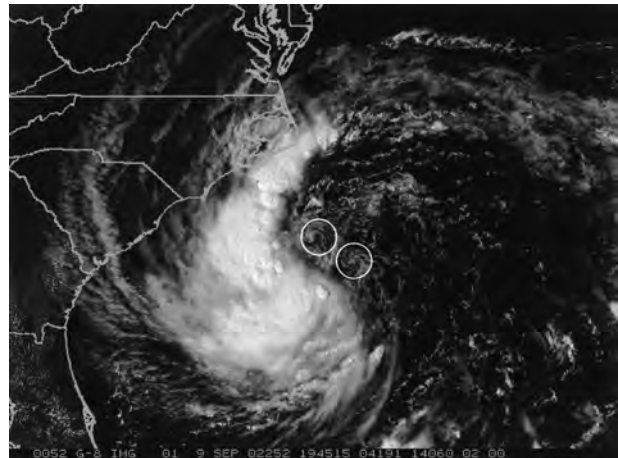


FIG. 4. Large-scale visible satellite image of Gustav at 1945 UTC 9 Sep 2002. The overshooting tops of multiple hot towers and two exposed mesovortices (denoted by white circles) are evident.

UTC 10 September (Fig. 1c). The QuikSCAT data indicate that the strongest low-level wind increase occurred between approximately 1200 UTC 10 September and 0000 UTC 11 September (Figs. 3c and 3d). The timing of the tropical transition cannot be determined explicitly because of the lack of temperature time history in the storm core and also the spatial uncertainty in the reanalysis fields. However, a warm core had probably formed by 1200 UTC 10 September, since this was the time of the most significant low-level wind spinup.

5. Mesoscale analysis

a. Observed convection

Having now summarized the synoptic-scale conditions, we turn our focus to the mesoscale and convective-scale conditions. Multiple hot towers (Riehl and Malkus 1958) were observed in Gustav on 9–10 September 2002. They are evident as overshooting tops in Fig. 4, along with two exposed mesovortices (discussed in section 5b). The hot towers are found to grow and die with lifetimes of approximately 0.5–1.0 h. The rapid scan imagery was used to obtain vertical velocity estimates in these towers, and vertically averaged (through the troposphere) updrafts of approximately 10 m s^{-1} were found. These were spatially and temporally averaged updrafts; therefore, velocities in excess of this value are expected to peak in the middle and upper tropospheres (e.g., Zipser and Gautier 1978; Zipser 2003) and in more localized regions. The deep convection initiated from an unstable moist air mass. The most

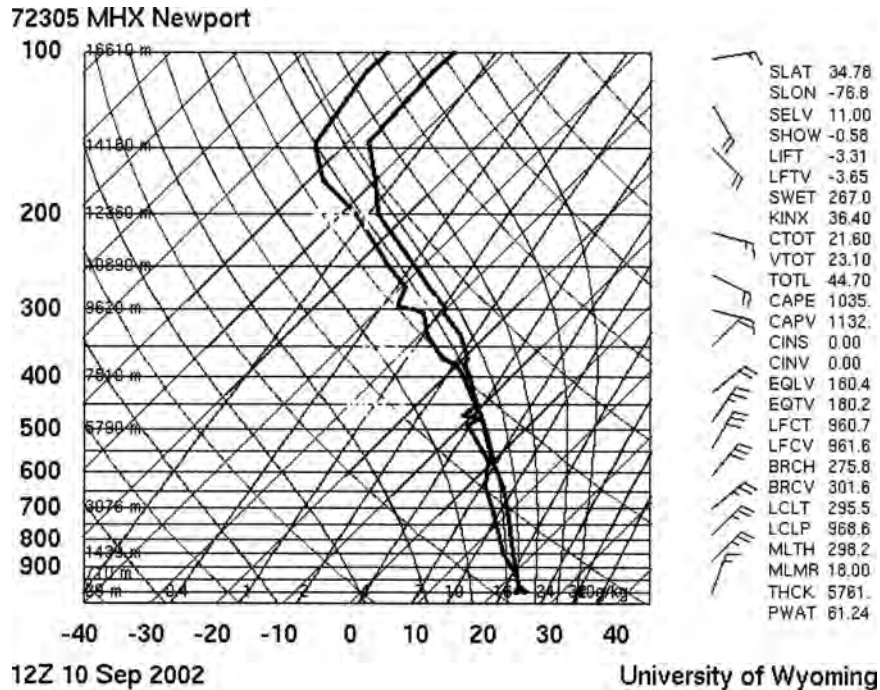


FIG. 5. Representative sounding of inflow air into Gustav on 10 Sep 2002 (courtesy of the University of Wyoming).

indicative sounding is the Newport, North Carolina (MHX), sounding at 1200 UTC 10 September, shown in Fig. 5. Mixed-layer CAPE (based on pseudoadiabatic parcel ascent using the mean values from 0 to 500 m) from this sounding is approximately 1000 J kg^{-1} .

b. Structure and evolution of mesovortices

Close-up images of Gustav are shown for 9 September in Fig. 6 at 1815 and 1945 UTC. Two distinct mesovortices are visible at each time, and a third one emerges just before dark (not shown). While there is no easy method for determining the horizontal scale of the mesovortices, they appear to be approximately 25–45 km in horizontal scale from their velocity signatures (low-level cloud swirls) in Fig. 6. The vorticity signatures of these mesovortices (or the horizontal extent of an isolated region of elevated vorticity) are likely smaller. For example, Reasor et al. (2005, hereafter RMB) found near-hurricane-strength low-level vorticity regions in prestorm Hurricane Dolly (1996) at very small scales (10–20 km) using airborne Doppler radar. The scales of the deep convective regions (defined by the width of the cloud shield just prior to the anvil stage) are approximately at the mesovortex (MV) scale (25–45 km; see Fig. 6). These mesovortices are found to emerge from underneath the deep convection and move with the low-level winds (Fig. 6, white arrows).

For example, at 1815 UTC, MV2 has just emerged from the sustained deep convective activity to the west. The exposure of the mesovortices from the convective towers is due to the moderate vertical shear at this time.

In summary, because, 1) the mesovortices are close to the same scale of the deep convective areas (Fig. 6), 2) there are no islands in the vicinity, and 3) they emerge as low-level circulations immediately *after* and *from underneath* the deep convective bursts, it is most likely that the mesovortices were generated via vortex stretching by updrafts in the deep convective cores. (This convective coupling is observed more clearly in an animation of the 7.5-min rapid scan imagery on 9 September; available online at <http://wx.met.nps.navy.mil/~mtmontgo/GustavAnimations/>.) The QuikSCAT data indicate that Gustav formed in a vorticity-rich environment, with a large area of near-surface absolute vertical vorticity greater than $2 \times 10^{-4} \text{ s}^{-1}$. This reservoir was likely utilized by the convective towers.

When Gustav became a tropical storm on 10 September, two more mesovortices were strikingly visible (Fig. 7, marked MV4 and MV5). The satellite imagery indicates that these mesovortices were rotating around one another from at least 1445 until 1900 UTC. At 1925 UTC, MV5 is no longer visible and MV4 appears to become the dominant vortex. A gigantic convective burst was initiated by MV4 with a circular exhaust

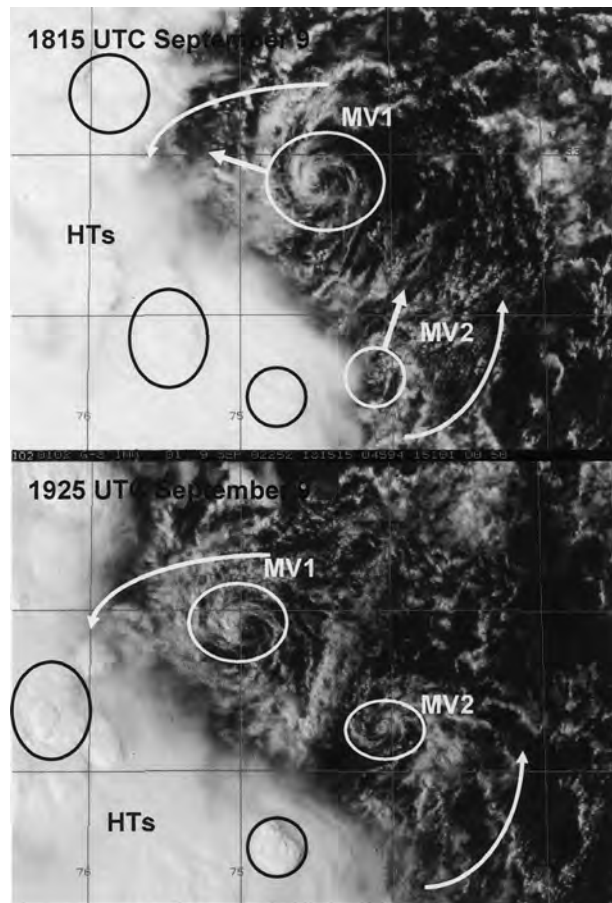


FIG. 6. *GOES-8* visible close-up depiction of mesovortices in Gustav at 1815 and 1945 UTC 9 Sep 2002. The overshooting convective tops associated with multiple hot towers are circled in black and marked HTs. The low-level exposed mesovortices are circled in white and marked with MV. The low-level motion of the MVs is shown by the white arrows. The approximate scales of the structures can be discerned from the scale of the latitude–longitude box: 32°–33°N (110 km) by 74°–75°E (94 km). The system-scale low-level circulation is shown by the white arrows.

cloud (CEC; Gentry et al. 1970) of horizontal scale of approximately 50–70 km (the early stages are shown at 1900 UTC in Fig. 7b). After this, sustained deep convection was present over the center of Gustav and the next day it was classified as a hurricane by the NHC. Due to the onset of darkness and increasing cloud cover, it is not known whether MV5 was expelled from the storm, merged into MV4, or dissipated. Subsequent to this, MV4 appeared to become the new circulation center, as has been shown in previous cases (cf. Stossmeister and Barnes 1992).

The convective generation of mesovortices is well documented in the literature (e.g., Marks et al. 1992; Stossmeister and Barnes 1992; Fritsch et al. 1994; RMB). Fritsch et al. (1994) demonstrated the formation

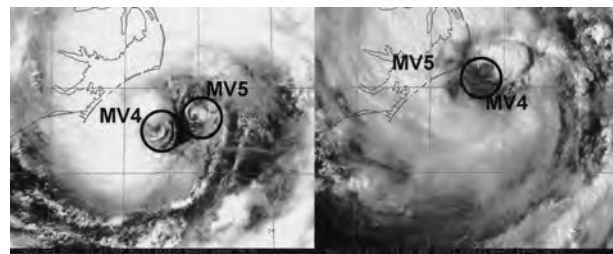


FIG. 7. Mesovortices in TS Gustav at (a) 1615 and (b) 1925 UTC 10 Sep 2002.

of a mesovortex (with an initial scale of approximately 100 km in diameter) over land via CAPE, without heat and moisture fluxes from the sea surface. Stossmeister and Barnes (1992) linked the formation of a second circulation center in Tropical Storm Isabel to intensifying deep convection in a rainband spiraling from the original center. RMB also demonstrated that the formation of circulations in the prehurricane Dolly disturbance likely proceeded via vortex tube stretching in association with hot tower convection.

These mesovortices form from a process different than that in mature hurricane eyewalls (Kossin and Schubert 2004). The latter are believed to form principally from a barotropic instability that necessarily requires a sign reversal of the local radial gradient of absolute vertical vorticity (Schubert et al. 1999). The Gustav mesovortices formed in an area where the vorticity distribution was approximately monotonic with radius from the circulation center, and thus formation by barotropic instability is not plausible.

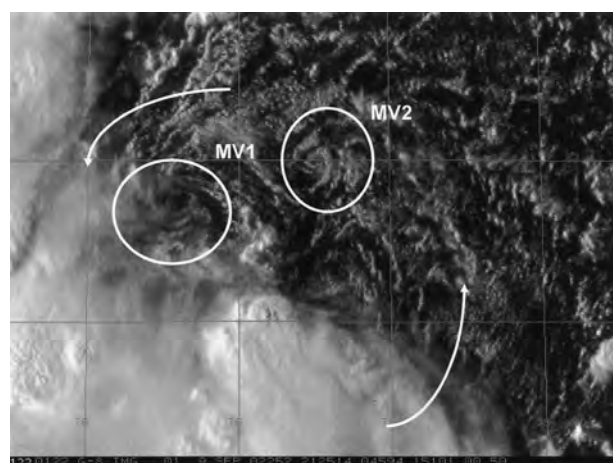


FIG. 8. The apparent axisymmetrization of a low-level mesovortex. At 2125 UTC 9 Sep 2002, MV1 appears to be strained and elongated from its earlier circular structure (image is brightened slightly to show the elongation of MV1). The system-scale low-level circulation is shown by the white arrows.

c. *Partial evidence of system-scale axisymmetrization*

The visible imagery provided partial evidence of the axisymmetrization of one mesovortex into the larger-scale vortex circulation (Fig. 8). As night began at 2125 UTC 9 September, MV1 appeared to be strained and elongated from its earlier circular structure (see Fig. 6). The straining and elongating of MV1 is consistent with the early phase of the axisymmetrization process of convectively generated vorticity anomalies leading to strengthening of the larger-scale (parent) vortex (Montgomery and Kallenbach 1997; Montgomery and Enagonio 1998; Melander et al. 1988; Dritschel and Waugh 1992). Based on available data, however, it is impossible to determine conclusively whether axisymmetrization of this anomaly occurred, since night fell and it moved underneath the convection. Shortly after MV1 moved underneath the convection, a large convective burst occurred over it, possibly indicating an intensification trend. MV1 was the only mesovortex that was observed to have strained and elongated.

6. Summary

Mesoscale and synoptic-scale observations of Tropical Storm Gustav were synthesized to provide a multiscale perspective of the tropical transition that occurred on 9–10 September 2002. On the mesoscale, rapid scan visible satellite imagery from *GOES-8* was used to illustrate and examine multiple mesovortices that existed in the storm on both of these days. The origin of these mesovortices was strongly suggested to be from vortex tube stretching due to their emergence from underneath deep convective regions soon after convective events. They became visible as low-level cloud swirls on 9 September due to easterly/southeasterly deep-layer shear of approximately $10\text{--}15\text{ m s}^{-1}$. Partial evidence of the axisymmetrization of one mesovortex into the parent vortex circulation was suggested with the rapid scan visible satellite imagery in the evening of 9 September. Two more mesovortices were visible on 10 September, while Gustav was a strong tropical storm. On both days, new hot towers were observed to form on the boundaries of existing mesovortices (MV1 on 9 September and MV4 on 10 September).

The synoptic-scale analysis of vertical wind shear, sea surface temperature, and moisture indicated that the environment was unfavorable for tropical cyclone formation on 9 September, but became favorable on 10 September. This was due to the concurrent relaxation of the 850–200-hPa vertical wind shear from $10\text{--}15$ to $5\text{--}10\text{ m s}^{-1}$ combined with storm movement over very

warm SSTs ($29.5^{\circ}\text{--}30.5^{\circ}\text{C}$) associated with the Gulf Stream. The spinup of near-surface winds from $10\text{--}15$ to $20\text{--}30\text{ m s}^{-1}$ from 1200 UTC 10 September to 0000 UTC 11 September (observed by QuikSCAT) indicates that the tropical transition of Gustav probably had been completed by this time. The QuikSCAT background absolute vertical vorticity was found to be approximately $1\text{--}2 \times 10^{-4}\text{ s}^{-1}$, with peak values of approximately $5\text{--}8 \times 10^{-4}\text{ s}^{-1}$. An accurate representation of the mesovortex vorticity was not possible since the QuikSCAT resolution was too coarse (25 km).

The observations presented herein are not sufficient to determine the precise role of the convective mesovortices in the tropical transition of Gustav. However, recent numerical simulations link warm core formation and tangential momentum spinup tendencies to these asymmetric eddy processes (MNCS; HMD; Montgomery and Enagonio 1998). Perhaps the most interesting aspect of this study is the illustration of the low-level complex flow patterns in a developing tropical cyclone, as well as the likelihood that convectively generated mesovortices exist in many tropical cyclones. Denser in situ observations and airborne Doppler radar will be necessary to observationally determine the relative importance of convective-scale eddy processes versus storm-scale mean processes and environmental factors in the genesis and intensification of tropical cyclones.

Acknowledgments. The authors thank R. Zehr and M. DeMaria of CSU/CIRA for providing the rapid scan visible satellite imagery of Tropical Storm Gustav (2002). We thank B. McNoldy of CSU for use of his QuikSCAT plotting algorithms. We thank L. Bosart, T. Vonderhaar, J. Vigh, and three anonymous reviewers for their helpful comments leading to improvements in the original manuscript. The NCEP–NCAR reanalysis data were provided by the NOAA–CIRES Climate Diagnostics Center, Boulder, Colorado (information online at <http://www.cdc.noaa.gov/>). The sea surface temperature plot, Fig. 2, was provided by the Space Department—Ocean Remote Sensing Group at the Johns Hopkins University Applied Physics Laboratory (<http://fermi.jhuapl.edu/index.html>). This research was supported by NSF ATM-0101781 and ATM-0132006.

APPENDIX

SeaWinds Scatterometer

The SeaWinds scatterometer is a microwave radar sensor used to measure the reflection or scattering effect produced while scanning the surface of oceans and gives an estimate of the near-surface winds. The instru-

ment provides measurements over an 1800-km swath during each orbit and covers 90% of the earth's oceans every day. Surface wind speeds are measured in the range of 3 to 20 m s⁻¹ with an accuracy of 2 m s⁻¹ for magnitude and 20 degrees for direction. The horizontal resolution of the retrieved wind vectors is 25 km. More information on the SeaWinds scatterometer can be found on the Internet Web site <http://winds.jpl.nasa.gov/> and more information on the level 3 gridded dataset from QuikSCAT can be found on the Internet Web site <http://podaac.jpl.nasa.gov/products/product109.html/>.

REFERENCES

- Beven, J., cited 2005: Tropical cyclone report: Hurricane Gustav. National Hurricane Center Archives. [Available online at <http://www.nhc.noaa.gov/2002gustav.shtml>.]
- Davis, C. A., and L. F. Bosart, 2003: Baroclinically induced tropical cyclogenesis. *Mon. Wea. Rev.*, **131**, 2730–2747.
- , and —, 2004: The TT problem: Forecasting the tropical transition of cyclones. *Bull. Amer. Meteor. Soc.*, **85**, 1657–1662.
- Dritschel, D., and D. Waugh, 1992: Quantification of the inelastic interaction of unequal vortices in two-dimensional vortex dynamics. *Phys. Fluids*, **4**, 1737–1744.
- Emanuel, K. A., J. D. Neelin, and C. S. Bretherton, 1994: On large-scale circulations in convecting atmospheres. *Quart. J. Roy. Meteor. Soc.*, **120**, 1111–1143.
- Fritsch, J. M., J. D. Murphy, and J. S. Kain, 1994: Warm core vortex amplification over land. *J. Atmos. Sci.*, **51**, 1780–1807.
- Gentry, R. C., T. J. Fujita, and R. C. Sheets, 1970: Aircraft, spacecraft, satellite and radar observations of Hurricane Gladys, 1968. *J. Appl. Meteor.*, **9**, 837–850.
- Gray, W. M., 1968: Global view of the origin of tropical disturbances and storms. *Mon. Wea. Rev.*, **96**, 669–700.
- Hendricks, E. A., M. T. Montgomery, and C. A. Davis, 2004: The role of “vortical” hot towers in the formation of Tropical Cyclone Diana (1984). *J. Atmos. Sci.*, **61**, 1209–1232.
- Kalnay, E., and Coauthors, 1996: The NCEP/NCAR Reanalysis 40-Year Project. *Bull. Amer. Meteor. Soc.*, **77**, 437–471.
- Kistler, R., and Coauthors, 2001: The NCEP–NCAR 50-year reanalysis: Monthly means CD-ROM and documentation. *Bull. Amer. Meteor. Soc.*, **82**, 247–267.
- Kossin, J. P., and W. H. Schubert, 2004: Mesovortices in Hurricane Isabel. *Bull. Amer. Meteor. Soc.*, **85**, 151–153.
- Marks, F. D., R. A. Houze, and J. Gamache, 1992: Dual-aircraft investigation of the inner core of Hurricane Norbert: Part I: Kinematic structure. *J. Atmos. Sci.*, **49**, 919–942.
- Melander, M. V., N. J. Zabusky, and J. C. McWilliams, 1988: Symmetric vortex merger in two dimensions: Causes and conditions. *J. Fluid Mech.*, **195**, 303–340.
- Montgomery, M. T., and B. F. Farrell, 1993: Tropical cyclone formation. *J. Atmos. Sci.*, **50**, 285–310.
- , and R. J. Kallenbach, 1997: A theory for vortex Rossby waves and its application to spiral bands and intensity changes in Hurricanes. *Quart. J. Roy. Meteor. Soc.*, **123**, 435–465.
- , and J. Enagonio, 1998: Tropical cyclogenesis via convectively forced vortex Rossby waves in a three-dimensional quasigeostrophic model. *J. Atmos. Sci.*, **55**, 2193–2200.
- , M. Nicholls, T. Cram, and A. Saunders, 2006: A “vortical” hot tower route to tropical cyclogenesis. *J. Atmos. Sci.*, **63**, 355–386.
- Reasor, P. D., M. T. Montgomery, and L. A. Bosart, 2005: Mesoscale observations of the genesis of Hurricane Dolly (1996). *J. Atmos. Sci.*, **62**, 3151–3171.
- Riehl, H., and J. S. Malkus, 1958: On the heat balance in the equatorial trough zone. *Geophysica*, **6**, 503–508.
- Schubert, W. H., M. T. Montgomery, R. K. Taft, T. A. Guinn, S. R. Fulton, J. P. Kossin, and J. P. Edwards, 1999: Polygonal eyewalls, asymmetric eye contraction, and potential vorticity mixing in hurricanes. *J. Atmos. Sci.*, **56**, 1197–1223.
- Sheets, R. C., 1990: The National Hurricane Center—Past, present, and future. *Wea. Forecasting*, **5**, 185–232.
- Stossmeister, G. J., and G. M. Barnes, 1992: The development of a second circulation center within Tropical Storm Isabel (1985). *Mon. Wea. Rev.*, **120**, 685–697.
- Zipser, E. J., 2003: Some views on “hot towers” after 50 years of tropical field programs and two years of TRMM data. *Cloud Systems, Hurricanes, and the Tropical Rainfall Measuring Mission (TRMM): A Tribute to Dr. Joanne Simpson*, Meteor. Monogr., No. 51, Amer. Meteor. Soc., 50–59.
- , and C. Gautier, 1978: Mesoscale events within a GATE tropical depression. *Mon. Wea. Rev.*, **106**, 789–805.